Bayesian Hierarchical Modeling of Nitrate Concentration in a Forest Stream Affected by Large-Scale Forest Dieback

Hoseung Jung[1], Cornelius Senf[1,2], Burkhard Beudert[3], and Tobias Krueger[1]

[1]IRI THESys & Geography Department, Humboldt-Universität zu Berlin, Berlin, Germany, [2]Ecosystem Dynamics and Forest Management Group, School of Life Sciences, Technical University of Munich, Munich, Germany, [3]Bavarian Forest National Park, Grafenau, Germany

Abstract The ecosystem function of vegetation to attenuate export of nutrients is of substantial importance for securing water quality. This ecosystem function is at risk of deterioration due to an increasing risk of large-scale forest dieback under climate change. The present study explores the response of the nitrogen (N) cycle of a forest catchment in the Bavarian Forest National Park, Germany, in the face of a severe bark beetle (*Ips typographus* Linnaeus) outbreak and resulting large-scale forest dieback using top-down statistical-mechanistic modeling. Outbreaks of bark beetle killed the dominant tree species Norway spruce (*Picea abies* (L.) H.Karst.) in stands accounting for 55% of the catchment area. A Bayesian hierarchical model that predicts daily stream NO_3 concentration (C) over three decades with discharge (Q) and temperature (T) (C-Q-T relationship) outperformed alternative statistical models. A catchment model was subsequently developed to explain the C-Q-T relationship in top-down fashion. Annually varying parameter estimates provide mechanistic interpretations of the catchment processes. Release of NO_3 from decaying litter after the dieback was tracked by an increase of the nutrient input parameter c_{s0}. The slope of C-T relation was near zero during this period, suggesting that the nutrient release was beyond the regulating capacity of the vegetation and soils. Within a decade after the dieback, the released N was flushed out and nutrient retention capacity was restored with the regrowth of the vegetation.

1. Introduction

Water is important in the global nutrient cycle, both as a transport agent and as a medium for biogeo-chemical reactions in soil, ground and surface waters. Large aquatic ecosystems rely on nutrient supply via hydrological pathways. However, when nutrients are present in water at excessive concentrations, they can cause environmental harm such as eutrophication and hypoxia, leading to deterioration of water quality for ecosystems and human use (Hilton et al., 2006; Xu et al., 2014). Vegetation is a crucial mediating agent in the cycling of water as it intercepts precipitation, and regulates evapotranspiration and groundwater flow (Adams et al., 2012; Harman et al., 2011). Nutrient exports are regulated by vegetation growth which assists in biogeochemical processes that retain or release nutrients in soils (Botter et al., 2010; Gall et al., 2013).

Forest catchments, whose hillslopes and riparian areas are covered largely by growing vegetation, are especially effective at regulating nutrient exports (Lajtha, 2020; Vitousek & Reiners, 1975). Since forests account for approximately 30% of global land cover (Hansen et al., 2013), the nutrient regulation of forest catchments provides a crucial ecosystem function for the conservation of water resources and ecosystems worldwide. In recent decades, concerns have grown about large-scale pulses of forest dieback due to drought and insect infestation (Allen et al., 2010; Seidl et al., 2017). Although tree mortality and pulses of increased mortality are natural processes, large-scale forest diebacks can result in excessive losses of nutrients and thus threaten ecosystem and drinking water quality (Gorham et al., 1979).

In a catchment experiencing pulses of increased forest mortality, export of nitrogen (N) is of key concern since inorganic nitrate (NO_3) is leached easily (Gundersen et al., 2006) and hence in-stream concentrations respond drastically to diebacks (Hartmann et al., 2016). Vitousek and Reiners (1975) were among the first to explain that an ecosystem loses nutrients after a forest dieback, but then retains them more effectively than before the dieback as biomass accumulates again during the following succession. Several studies have since observed increases of inorganic N exports in forest catchments affected by forest diebacks caused by bark beetle infestation (Beudert et al., 2014, 2016), wildfire (Betts & Jones, 2009), windthrow (Hartmann

et al., 2016) and also in watersheds affected by clear-cut harvest (Pardo et al., 1995). The temporal evolution of the processes regulating and exporting N, however, remain poorly quantified.

The European spruce bark beetle (*Ips typographus* Linnaeus) is one of the most important biotic disturbance agents in Central Europe (Schelhaas et al., 2003; Seidl et al., 2014). It occurs throughout the whole range of its host tree, Norway spruce (*Picea abies* (L.) H.Karst.), having widespread ecological and economic impacts (Hlásny et al., 2019). Outbreaks of the European spruce bark beetle have increased in frequency and magnitude across Europe over recent decades (Seidl et al., 2014), leading to unprecedented large-scale diebacks of Norway spruce in many regions (Senf & Seidl, 2018). Yet, recent studies have shown that forests in Central Europe have been highly resilient to recent outbreaks, with trees returning after several years post dieback (Senf et al., 2019; Zeppenfeld et al., 2015). In order to quantify the effect of bark beetle induced forest diebacks on a catchment's N cycle, it is thus important to (i) improve our mechanistic understanding of how bark beetle induced forest dieback affects N cycles, and (ii) understand the effect of both dieback and recovery on N cycles over long time periods. Achieving these goals requires a novel modeling approach and the integration of various data sources.

Nutrient export from a catchment is complicated by heterogeneous sources, dynamic pathways and variable biogeochemical processes (Basu et al., 2011; Musolff et al., 2015). It is challenging to monitor the relevant processes in hillslopes and streams across an entire catchment. In practice, nutrient concentration is most often monitored in streams representing integrated effects of catchment processes and enabling quantification of downstream export. The relationship of solute concentration with discharge (C-Q relationship) and its variation in space and time has proven a particularly useful indicator of catchment processes (Musolff et al., 2015; Rose et al., 2018; Zhi et al., 2019). Previous studies showed that the C-Q relationship is determined by the reactivity of the solute and the spatial correspondence between source areas and runoff (Basu et al., 2011; Seibert et al., 2009; Thompson et al., 2011). These studies have followed a data-driven, or "top-down" modeling approach (Sivapalan et al., 2003) that aims at accounting for the dominant catchment processes using parsimonious model structures that are commensurate with the often limited availability of data (Krueger et al., 2007). Such parsimonious hydrochemical models often picture a catchment as a single unit in which transport and biogeochemical reactions of solutes are conceptualized without explicit explanation of their spatial heterogeneity.

Regression models have proven particularly efficient in screening and investigating the relationships of nutrient concentrations with other environmental variables (Chavez & Service, 1996; Clark et al., 2004; Exner-Kittridge et al., 2016). Where these data and relationships relate to disparate scales then a hierarchical model is called for, with the Bayesian hierarchical framework being the most flexible and coherent. The Bayesian approach offers more straight-forward interpretation of model uncertainties and more flexible models. Bayesian hierarchical modeling has been applied to hydrochemical data to predict the behavior of aquatic environments such as nutrient concentrations (Xia et al., 2016), algal blooms (Cha et al., 2016, 2017; Obenour et al., 2014), dissolved oxygen (Borsuk et al., 2001; Stow & Scavia, 2008) and salinity (Webb et al., 2010). Borsuk et al. (2001) and Stow and Scavia (2008) applied mechanistic models in a Bayesian hierarchical framework combining the strengths of mechanistic and statistical modeling; making predictions based on process knowledge while estimating parameters empirically from data. The relationships between variables revealed by statistical models can indeed inspire parsimonious mechanistic models and therefore assist understanding of hydrochemical processes. Parsimonious models aim at describing the dominant processes controlling nutrient cycling tuned to the predictors at hand, whereby the Bayesian hierarchical framework allows missing processes to be represented by "random effects" across multiple temporal or spatial units. This approach allows understanding to be gained and predictions to be made with the available data while prompting further experimentation and data collection to eventually explain and replace random effects with mechanistic equations.

The aim of this study was to investigate the three-decade long response of a catchment's N cycle to bark beetle induced forest dieback using in-stream monitoring data and Bayesian hierarchical modeling in a top-down fashion. Our study catchment is the Grosse Ohe catchment in the Bavarian Forest National Park in Germany. The Bavarian Forest National Park has experienced two large-scale bark beetle outbreaks between 1990 and 2010 (Kautz et al., 2011), which led to the dieback of most of the bark beetle's host trees. As the bark beetle outbreaks were not managed, the catchment provides a unique opportunity for studying

the effects of bark beetle induced forest dieback, and the following recovery of vegetation, on N cycling. Specifically, we set out to analyze how the nutrient retention capacity of the forest catchment was affected by large-scale tree mortality, both during and after the dieback. To this end we first developed a Bayesian hierarchical model through state-of-the-art model comparison to investigate temporally variant relationships between stream NO_3 concentration and available environmental variables. Second, the resultant model structure inspired a parsimonious catchment model that provides mechanistic interpretations of catchment dynamics across sites and years. The derivation of the parsimonious catchment model, resulting from the initial Bayesian hierarchical model, will be described in the results section. We conclude our analysis by correlating model parameters with an independent remote sensing based proxy of vegetation activity, the normalized difference vegetation index (NDVI) in order to guide parameter interpretation and independently evaluate the plausibility of the mechanistic model.

2. Materials and Methods

2.1. Study Area and Measurements

Grosse Ohe is a headwater catchment located in the Bavarian Forest National Park, Germany, with a size of 19.1 km^2 and a mountainous topography with 11.1° mean slope at altitudes of 770–1,447 m above sea level. Ninety-eight percent of the catchment area is forested, and human management was excluded since at least the 1970s (i.e., since establishment of the National Park). Norway spruce dominated forests cover approximately 70% of area, with the remaining area being dominated by European beech (*Fagus sylvatica* L.). Stream hydrochemistry was monitored at the outlets of Grosse Ohe (48°56′17.99′′ N, 13°24′45.13′′ E) and its two nested subcatchments Markungsgraben (48°57′20.89′′ N, 13°25′35.8′′ E, 1.1 km^2) and Forellenbach (48°56′33.61′′ N, 13°25′10.63′′ E, 0.7 km^2). The forest dieback was most severe in Markungsgraben (mortality on approximately 82% of the catchment area) compared to Forellenbach (mortality on approximately 57% of the area) and the entire catchment Grosse Ohe (mortality on approximately 55% of the area). A map displaying the study catchment with the forest dieback, the streams and the monitoring stations can be found in Figure S1 of the Supporting Information.

The hydrochemical measurements include water level and concentrations of nitrogen (N) and phosphorus (P) species, organic carbon and dissolved oxygen (DO), pH, conductivity and water temperature. Water levels were measured quasicontinuously (every 15 min) and converted to discharges via rating curves. The rating curves were developed based on current meter data in Forellenbach and Grosse Ohe and salt dilution data in Markungsgraben (Beudert & Gietl, 2015). Baseflow was separated from total discharge with a digital filter algorithm available in the R package "EcoHydRology" (Fuka et al., 2018). The baseflow index was computed as the proportion of baseflow relative to discharge. Instantaneous samples for chemical analyses were taken manually every two weeks at Grosse Ohe and Markungsgraben and weekly at Forellenbach. The samples were analyzed monthly in the laboratory to determine nutrient concentrations according to DIN/EN/ISO. Temperature, pH, DO and electric conductivity were measured on subdaily basis, and were aggregated to daily means to be matched with the instantaneous sample data for congruent analysis. The monitoring programs started in 1977 for Grosse Ohe, 1988 for Markungsgraben and 1990 for Forellenbach. Water temperature was only available from 2002 and DO was not available at Forellenbach. Further details of the geographical and hydrometeorological characteristics and monitoring of the area are described in Beudert and Gietl (2015).

The annual percentage of forest canopy experiencing dieback was manually identified via airborne image analysis (see Heurich et al. (2010) for details). We further acquired annual normalized difference vegetation index (NDVI) time series from the United States Geological Survey Landsat satellite archive for the years 1986–2016 (see Senf et al. (2017) for details on image processing). We used the NDVI time series as independent proxy of vegetation activity, that is, indicating the loss and subsequent recovery of photosynthetic activity during and after the bark beetle outbreak. We averaged annual NDVI observations at the catchment level and applied a smoothing model (generalized additive model) to account for variable phenology between Landsat acquisitions that potentially overshadow the more subtle longer-term trends associated with forest dieback and recovery (Senf et al., 2019).

2.2. Bayesian Hierarchical Model

The concentrations of NO_3 in the streams of Grosse Ohe and its nested subcatchments were predicted by regression models in a Bayesian hierarchical framework. Candidate regression models with different sets of predictors were compared (see below). The slopes and intercepts of these models were allowed to vary for each hydrological year (starting in November):

$$\log(C_i) = \beta_{0,j} + \beta_{1,j}X_{1,i} + \beta_{2,j}X_{2,i} + \cdots + \beta_{P,j}X_{P,i} + \varepsilon_i \tag{1}$$

where C_i and $X_{\{1,2,\ldots,P\},i}$ are ith measurements of stream NO_3 concentration and the corresponding values of the P predictors, respectively. $\beta_{0,j}$ and $\beta_{\{1,2,\ldots,P\},j}$ are the intercept and slope parameters for the P predictors, respectively, for the jth year. ε_i is the residual error. By modeling ε_i as a normal distribution and taking the logarithm of the response C_i, NO_3 concentration was effectively modeled as a lognormal distribution. The model parameters $\beta_{0,j}$ $\beta_{\{1,2,\ldots,P\},j}$ and variance $\sigma_{\varepsilon_j}^2$ of ε_i were partially pooled across the hydrological years to control overfitting. That is, these parameters were modeled as realizations of common distributions, whose parameters were simultaneously inferred from the data:

$$\beta_{m,j} \sim \text{Normal}\left(\mu_{\beta_m}, \sigma_{\beta_m}^2\right), \text{for } m = 0,1,2,\ldots P \tag{2}$$

$$\varepsilon_i \sim \text{Normal}\left(0, \sigma_{\varepsilon_j}^2\right) \tag{3}$$

$$\sigma_{\varepsilon_j} \sim \text{Normal}\left(\mu_{\sigma_\varepsilon}, \sigma_{\sigma_\varepsilon}^2\right) \tag{4}$$

where μ_{β_m} is the mean of the regression parameter β_m and $\sigma_{\beta_m}^2$ is the variance of the "random effect" that models the variability of β_m between years.

The residual error ε_i is considered normally distributed with mean zero and variance $\sigma_{\varepsilon_j}^2$, which varies between years according to another, common normal distribution with mean μ_{σ_ε} and variance $\sigma_{\sigma_\varepsilon}^2$. Weakly informative Normal $(0,5)$ prior distributions were assigned to μ_{β_m}. Weakly informative Inverse-gamma $(0.01, 0.01)$ priors were assigned to σ_{β_m}, μ_{σ_ε} and $\sigma_{\beta_\varepsilon}$ as these parameters are bound to be positive (Gelman, 2006). The prediction of NO_3 was not sensitive to the prior distributions; results of a sensitivity analysis are displayed in Figure S3 of the Supporting Information. Allowing the parameters and residual error term to vary temporally in the Bayesian hierarchical framework reflects the possibility that the processes that regulate stream NO_3 vary over time, but shrunk toward a common mean. From this temporal variation of model parameters we extract information on catchment dynamics in top-down fashion (see Section 2.3).

A variant of the Weighted Regression against Time, Discharge, and Season (WRTDS) model by Hirsch et al. (2010) was included as a candidate model to assess the effect of seasonality on NO_3 export. This model, hereafter called the C-Q-S model, was implemented in the Bayesian hierarchical framework by adding the two-parameter sinusoidal function of day of the WRTDS model to the C-Q model.

The partially pooled models were compared with pooled and nonpooled models. In the pooled version, all parameters were constant over the years. In the nonpooled version, all parameters were estimated individually for each year, without common prior distributions. The joint posterior distribution of the parameters was simulated using Markov Chain Monte Carlo (MCMC) methods available in Stan (Carpenter et al., 2017) and implemented in the R environment (R Core Team, 2018; Stan Development Team, 2018). Two thousand realizations of the model parameters and predicted NO_3 were generated from their posterior distributions after 2,000 warmup samples in four parallel chains. The MCMC chains for all parameters of all models converged with $\hat{R}$ ranging 0.99–1.02. Code files of the partially pooled, nonpooled and pooled models are provided in the Supporting Information.

The candidate regression models with different sets of predictors were compared for their out-of-sample predictive accuracy by means of k-fold cross validation. The data sets of each site were randomly divided into 10 subsets y_k, for $k = 1, 2, \ldots, 10$, with even numbers of data point. The models were fit to a training data

set $y_{(-k)}$, i.e., with the kth subset left out, and subsequently used for predicting the NO_3 concentrations of the validation set y_k. This process was repeated for each subset and the posterior distributions of the predictions were used to calculate the expected log pointwise predictive density (ELPD), a relative measure of predictive performance under out-of-sample conditions (Vehtari et al., 2017). ELPD in a k-fold cross validation is computed with S simulation draws from the posterior predictive densities using the following equation.

$$\text{ELPD} = \sum_{i=1}^{n} \log\left(\frac{1}{S} \sum_{s=1}^{S} p\left(y_i \mid \theta^{k,s} \right) \right) \tag{5}$$

where n is the number of data points, $p\left(y_i \mid \theta^{k,s} \right)$ is the predictive density of the ith data point using the simulations corresponding to the validation set k that contains that data point, $\theta^{k,s}$ is the sth draw of the posterior parameter density based on training set $y_{(-k)}$. We calculated k-fold cross validation ELPD instead of leave-one-out (LOO) cross validation ELPD because of the number of data points in this study which overwhelmed the LOO algorithm; see Vehtari et al. (2017) for a comparison and discussion.

2.3. Top-Down Catchment Model

In a second step, the regression analysis (Section 2.2) was interpreted with a parsimonious process-based model of NO_3 export at the catchment scale in top-down fashion (Sivapalan et al., 2003). Equations describing the processes of nutrient export were defined using the predictor variables of the best fit regression model and the literature. In this way, mechanistic implications of the regression model were derived. Lastly, as a first step toward explaining the temporal variation of the parameters in relation to the bark beetle induced forest dieback, correlations between annual parameter estimates and the NDVI as independent proxy of vegetation activity were quantified using Spearman's rank correlation coefficient (ρ).

3. Results

3.1. Temporal Variations of Vegetation Canopies and Hydrochemical Responses

Over the entire catchment, Grosse Ohe, the bark beetle infestation occurred in two waves between 1994 and 2009. The canopy cover of vital spruce was reduced at maximum annual rates in 1999 and 2006 (12% year and 5% of the catchment area, respectively) (Figure 1a). The infestation occurred in Forellenbach in 1994–2000 and 2002–2008 with maximum annual mortalities of 12% (1999) and 7% (2006), respectively. The bark beetle outbreak led to highest mortality rates in the Markungsgraben catchment between 1995 and 2001, where a maximum annual mortality rate of 39% was recorded in 1997. The declines in annual NDVI time series lagged 3 years behind the dieback in Markungsgraben and coincided with the second dieback in Forellenbach and Grosse Ohe. The largest negative deviations in annual NDVI (i.e., annual vegetation activity) were found in Markungsgraben (Figure 1a), but with rapid recovery of vegetation activity after the main mortality waves for all catchments. The rapid return of vegetation is also well documented in other studies (Senf et al., 2019; Svoboda et al., 2010; Zeppenfeld et al., 2015), which report that recovery is mainly driven by natural regeneration of spruce trees, as opposed to pioneer or broadleaved species. The tree community thus did not change significantly over the bark beetle outbreak. We however note that the NDVI is likely also influenced by understory vegetation utilizing the greater light availability after the dieback of the top canopy (Hais et al., 2009).

Discharge was highly variable over the course of the bark beetle outbreaks (Figure 1b), with a discharge yield of 0.40–58.5 mm day^{-1} across all sites and over the entire monitoring period. In volumetric terms, the largest flux occurred at the most downstream monitoring station of Grosse Ohe (0.59 ± 0.66 m^3 s^{-1} (mean ± standard deviation)), followed by the upstream stations Markungsgraben (0.05 ± 0.06 m^3 s^{-1}) and Forellenbach (0.02 ± 0.02 m^3 s^{-1}). The baseflow indices were 64%, 54% and 49% in Forellenbach, Grosse Ohe and Markungsgraben, respectively. The baseflow contribution decreased with increasing mean slope (8.4° in Forellenbach, 11.1° in Grosse Ohe and 16.1° in Markungsgraben). Neither annual mean nor high flow (95th percentile) showed a significant trend over the years, or response to the disturbance, at any of the sites (Mann-Kendall test p > 0.05).
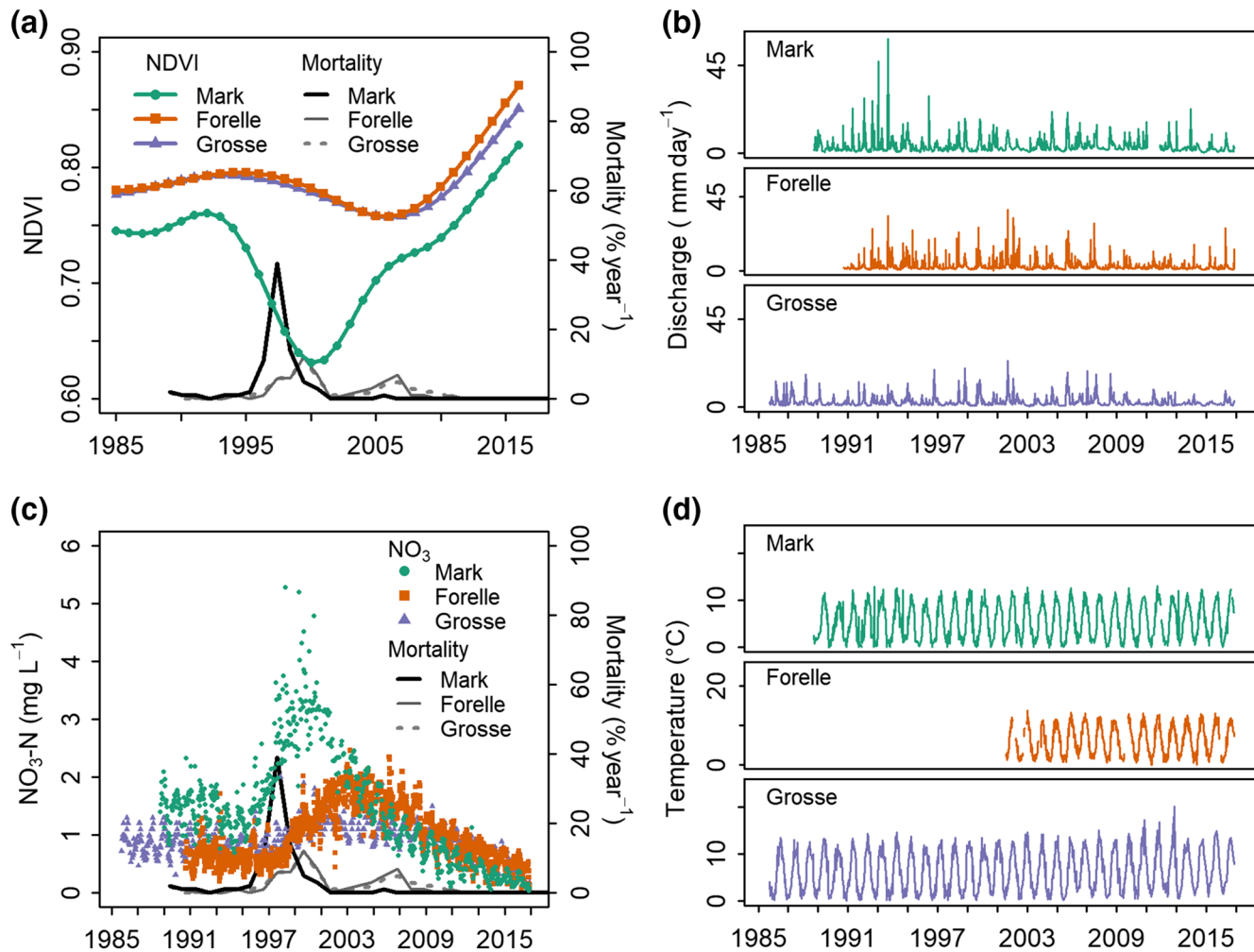
Figure 1. (a) Normalized difference vegetation index (NDVI) and mortality, (b) discharge, (c) nitrate concentration and mortality (NO₃), and (d) water temperature of subcatchments Markungsgraben (Mark) and Forellenbach (Forelle) and the entire catchment Grosse Ohe (Grosse).

Annual mean stream NO_3 concentration increased during the dieback periods (1.56–3.33 mg N L^{-1} in 1995–2000 at Markungsgraben, 0.63–1.84 mg N L^{-1} in 1998–2003 at Forellenbach and 0.59–1.84 mg N L^{-1} in 1995–2003 at Grosse Ohe) (Figure 1c). NO_3 was the major N species in the streams, where its mean concentration was two to three orders of magnitude and 15–44 times higher than that of nitrite (NO_2) and ammonium (NH_4), respectively, across the sites. Spearman's rank correlation coefficients ρ between annual mean NO_3 and NDVI were −0.88–−0.82 across the sites, meaning that stream NO_3 decreased when the vegetation was active (compare Figures 1a and 1c). We note that the temporal trend of NO_3 lagged 3–4 years behind that of the NDVI in Forellenbach and Grosse Ohe. NO_3 showed minima in the growing season (May–September) and maxima in the dormant season. However, under elevated NO_3 concentrations during the dieback, the seasonal pattern vanished in 2004 at Forellenbach and in 1998 and 2003 at Markungsgraben. We define the years with decreased NDVI and elevated NO_3 (1995–2003 at Markungsgraben, 1997–2009 at Forellenbach and Grosse Ohe) as the dieback phase and the preceding and following years as the pre and postdieback phases, respectively. Annual NO_3 load exported from the (sub) catchments increased during the dieback phase, and tended to decrease in the postdieback phase lower than predieback levels (Table S1).

The water temperature ranged between −0.01 and 20.1°C, while 95% of the values were within 0.03–13.0°C, with means increasing above 5°C in May–October (Figure 1d). Temperature measurements at the three sites were highly correlated ($p < 0.01$, r^2 0.83–0.96). Annual mean temperatures showed clear and steady increasing trends across the sites (Mann-Kendall test $p < 0.05$).

3.2. Selection of Regression Model

The regression models with different sets of predictors and pooling setups were compared using ELPD, with greater values signifying better predictive performance. Both original and log-transformed data were tested, and the ELPDs of the best fitting models are presented in Table S2 of the Supporting Information. The C-Q-T (concentration-discharge-temperature) model with partially pooled parameters showed the highest ELPD values across the sites, outperforming even models with three predictors. The C-Q-DO model (concentration-discharge-dissolved oxygen) was more accurate than the C-Q-T model at Grosse Ohe but the enhancement in ELPD was low (0.01). The C-Q-T-DO (concentration-discharge-temperature-dissolved oxygen) model showed reduced accuracy compared to the C-Q-T and the C-Q-DO models, suggesting confounding effects of temperature and DO and thus overfitting. DO was correlated with water temperature with $\rho = -0.72$ at Markungsgraben and $\rho = -0.97$ at Grosse Ohe because of the increased solubility of oxygen in water at low temperatures (Wetzel, 2001). No DO data were available for Forellenbach. The C-Q-S model showed lower predictive accuracy than the C-Q-T and C-Q-DO models, possibly because temperature and DO represented more efficiently the seasonality of nutrient uptake than the sinusoidal function or due to overparameterization as it has one more parameter than the other models.

As a result, the C-Q-T model was selected for further analysis. The equation can be written as

$$\log\left(C_i\right) = \beta_{0,j} + \beta_{1,j} \cdot \log Q_i + \beta_{2,j} \cdot T_i + \varepsilon_i \tag{6}$$

3.3. Development of Top-Down Catchment Model

A mechanistic model explaining the variation of in-stream NO_3 with discharge and water temperature was developed based on the relationships between the variables suggested by the selected regression model. This model is a lumped model that conceptualizes the processes within the catchment as a single unit. Hence the parameters of this model represent the characteristics of the entire catchment without spatial heterogeneity; they are so called "effective" parameters.

The high accuracy of the C-Q-T and C-Q-DO models as well as Hirsch et al. (2010) suggest that the NO_3 export was determined by the seasonal pattern of biogeochemical reactions in the catchment. Vegetation retains more nutrient in summer as it grows at an increased rate induced by a rise in temperature (Pregitzer & King, 2005) and loses nutrient via litterfall (Kaiser et al., 2011). The high correlation between water temperatures at the three sites (Section 3.1) implies that the water temperature reflects the regional climate of the area. Accordingly, we use water temperature as a surrogate variable that represents soil and water temperatures of the entire catchment.

The linear relationship of $\log(NO_3)$ and temperature in the regression model (Equation 6) suggests that NO_3 is processed in first-order reactions with rates affected by temperature. In the soil of the catchment, including hillslope, riparian and hyporheic zones, the NO_3 is either removed by assimilation of plants and microorganisms or by denitrification, or produced from organic N via mineralization and nitrification (Stoddard, 1994; Zheng et al., 2016). NO_3 concentration at the soil surface (c_s [mg N L^{-1}]) may thus be modeled by first-order reaction with its rate proportional to temperature T`:

$$\frac{dc_s}{dt} = kT`c_s \tag{7}$$

where k (C$^{\circ -1}$ s^{-1}) is the rate constant. Integrating this differential equation over the retention time of NO_3 in the surface layer (t_r [s]) gives the following exponential function of c_s:

$$c_s = c_{s0} \cdot e^{kt_r \overline{T`}} \tag{8}$$

where $\overline{T`}$ is the mean soil temperature during the residence time and $c_0$ (mg N L$^{-1}$) is the initial concentration of $NO_3$ input. We take $T$, the stream water temperature, as surrogate for $\overline{T`}$, which varies instantaneously at the scale of t_r.

The vertical concentration profile of NO_3 in the soil is shaped by the heterogeneities of the biogeochemical reactions and retention times. NO_3 concentration at depth z may be expressed as

$$c_z = c_s \cdot e^{fz} \tag{9}$$

Inserting Equation 8 into Equation 9 yields

$$c_{z,T} = c_{s0} \cdot e^{kt_r T + fz} \tag{10}$$

where $f (\mathrm{m^{-1}})$ is the shape parameter of the NO_3 depth profile. The biogeochemical processes were assumed to alter the NO_3 concentration in the soil instantaneously or within the residence time t_r before the nutrient is discharged via the stream (Seibert et al., 2009). The seasonal variation of NO_3 is formed by litterfall (Kaiser et al., 2011) and biogeochemical reactions that take place most actively in the near-surface layer of the soil (Chen et al., 2005). $kt_r T$ represents the reactions in this layer with the rates affected by temperature, although the thickness of the layer cannot be determined with current site knowledge. The depth profile modulated by f accounts for additional spatial heterogeneity of nutrient input, residence time and reaction rate.

NO_3 is assumed to be transported laterally from the soil to reach the stream. Lateral water flux at depth z, q $(\mathrm{m^2\ s^{-1}})$, was modeled to decline exponentially (Seibert et al., 2009):

$$q = q_0 \cdot e^{\lambda z} \tag{11}$$

where $\lambda\ (\mathrm{m^{-1}})$ is a shape parameter of the water flux profile and $q_0\ (\mathrm{m^2\ s^{-1}})$ is the transmissivity at the top of the soils. The hydraulic conductivity of the soil was assumed to be little affected by the forest dieback and thus was not modeled to change over the years.

Integration of Equation 11 over z results in an equation for discharge $(\mathrm{m^3\ s^{-1}})$ governed by groundwater depth, or depth of the saturated zone below the soil surface:

$$Q = q_0 / \lambda \cdot e^{\lambda z} \tag{12}$$

$q_0/\lambda\ (\mathrm{m^3\ s^{-1}})$ represents the maximum discharge when the soil is saturated (groundwater depth $z = 0$ m), neglecting overland and preferential flows.

Modifying the model by Seibert et al. (2009) to average the NO_3 flux (concentration; Equation 10) times lateral water flux (Equation 11) over depth results in a governing equation of in-stream NO_3 concentration as a function of soil inputs (represented by c_{s0}), discharge (Q) and temperature (T):

$$C = \frac{L}{Q} = \frac{\int_{-\infty}^{z_t} qc_z dz}{\int_{-\infty}^{z_t} q dz} \tag{13}$$

$$\begin{aligned} \log C &= \log\left[c_{s0}(1+b)^{-1}\left(\frac{\lambda}{q_0}\right)^b \right] + b \cdot \log Q + kt_r T \\ &= \log S + b \cdot \log Q + kt_r T \end{aligned} \tag{14}$$

where z_t is ground water depth at time t, b is f/λ (-) and S is $c_{s0}(1+b)^{-1}(\lambda / q_0)^b$. See Supporting Information Text S1 for a detailed derivation of Equation 14 from Equation 13. Equation 14 combines the C-Q and C-T relationships into the C-Q-T relationship revealed by the best fit regression model. The rationale of the current model explains the mechanism of the empirical C-Q-T relationship. While Seibert et al. (2009) attributes the C-Q relationship to a heterogeneous distribution of the solute in the riparian zone, the current study adapted the model assuming that the spatial distribution in the soil over the entire catchment determines the relationship (Basu et al., 2010; Musolff et al., 2016; Thompson et al., 2011). Parameters $\log S$, b and kt_r were read from the regression intercept and coefficients estimated by MCMC as explained in Section 2.2. In what follows, these parameters will be interpreted by the elaborations the mechanistic model provides.

From the definition of S it follows that

$$c_{s0} = S(1+b)(q_0 / \lambda)^b \qquad (15)$$

This equation can be used for estimating c_{s0}, which is affected by the dynamics of the vegetation and hence potentially sensitive to the bark beetle outbreak.

It is important to note that Equations 6 and 14 are analogous to each other. The intercept of the regression model is log$S$, a compound of four mechanistic parameters; c_{s0}, b, λ and q_0. S is thus proportional to NO_3 input concentration (c_{s0}). This parameter also has a positive or negative relationship with the maximum discharge (q_0/λ) depending on the sign of b. The slopes of Equation 6, β_1 and β_2, correspond to b ($=f/\lambda$) and the product of k and t_r of Equation 14 (kt_r), respectively. In our hierarchical setup, these parameters are allowed to vary between years. The soil input c_{s0} can be inferred from the annual estimates of S and b given values of q_0 and λ. The C-Q slope b signifies the vertical profile of NO_3 transport through the soil shaped by hydraulic conductivity (λ) and availability of the nutrient (f). A positive k indicates that the catchment is a source of NO_3 and a negative k indicates a sink, while t_r is always equal to or larger than zero. Accordingly, the parameter kt_r represents the rate of removal ($kt_r < 0$ C$^{\circ-1}$) or production ($kt_r > 0$ C$^{\circ-1}$) of NO_3 in the soil surface. The magnitude of net removal/production is determined both by the biogeochemical reaction (k) and the residence time (t_r). With $kt_r < 0$ C$^{\circ-1}$, NO_3 is lower in summer creating a seasonal pattern because high temperature enhances net NO_3 removal (Christensen et al., 1990; Clark et al., 2004; Huber, 2005). The seasonal pattern is reversed if $kt_r > 0$ C$^{\circ-1}$ with net NO_3 production magnified by a temperature increase.

3.4. Prediction of Nitrate

The stream NO_3 concentrations predicted by the C-Q-T model corresponded well with the observed concentrations (Figure 2). The root mean square errors (RMSE) were 0.36 (0.33–0.40) (mean [95% credible interval]) mg N L^{-1}, 0.20 (0.19–0.22) mg N L^{-1} and 0.18 (0.17–0.19) mg N L^{-1} across the years at Markungsgraben, Forellenbach and Grosse Ohe, respectively. The model predicted the seasonal pattern of NO_3 correctly, as well as the disappearance of the seasonal pattern in the dieback phase at Markungsgraben (1997–2001) and Forellenbach (2002). In these years, the two predictors were insufficient to explain the NO_3 dynamics, showing higher RMSEs (0.68 [0.58, 0.80] mg N L^{-1} at Markungsgraben and 1.10 [0.98, 1.19] mg N L^{-1} at Forellenbach). At Forellenbach, NO_3 often decreased sharply at high flows due to dilution. Prediction of NO_3 and further data analysis could not be performed before 2002 at Forellenbach due to the limited availability of temperature data.

Plotting predicted and observed in-stream NO_3 against each other verified the high predictive accuracy of our model (Figure 3). The RMSE normalized by the mean of observed NO_3 indicated that the deviation between the predicted and observed NO_3 was lowest at Forellenbach, followed by Grosse Ohe and Markungsgraben. The model was not able to explain the variation of NO_3 (showing high RMSE) and tended to underestimate the nutrient concentration in the years when the nutrient concentration peaked.

3.5. Temporal Variations of Model Parameters

The parameter S was estimated for each year by exponentiating the intercept of the regression model based on Equation 14 (Figure 4a). S was greatest at Markungsgraben (annual median of 0.08–5.15 mg N L^{-1}), where the NO_3 concentration was generally highest, compared to the medians of 0.05–1.97 mg N L^{-1} at Forellenbach and 0.40–1.80 mg N L^{-1} at Grosse Ohe. S showed a temporal pattern similar to that of annual mean in-stream NO_3 across the sites with an annual median ρ of 0.77–0.94, increasing in the dieback phase and decreasing in the postdieback phase. Since S is a complex of multiple parameters (Equation 14), we will describe the temporal dynamics further in terms of c_{s0} below (see Equation 15).

The parameter kt_r was significantly (P($kt_r > 0$ C$^{\circ-1}$) < 0.05) below zero in the pre and postdieback phases. kt_r increased to approach zero in some years in the middle of the dieback phase (Markungsgraben in 1997–1999, Forellenbach in 2003–2004 and 2007) (Figure 4b). At Grosse Ohe, the 95% credible intervals of kt_r remained below zero throughout the study period. The annual medians of kt_r at Forellenbach and Grosse Ohe remained in the ranges of −0.06–0.00°C^{-1} and −0.04–−0.02°C^{-1}, respectively. The kt_r at Markungsgraben
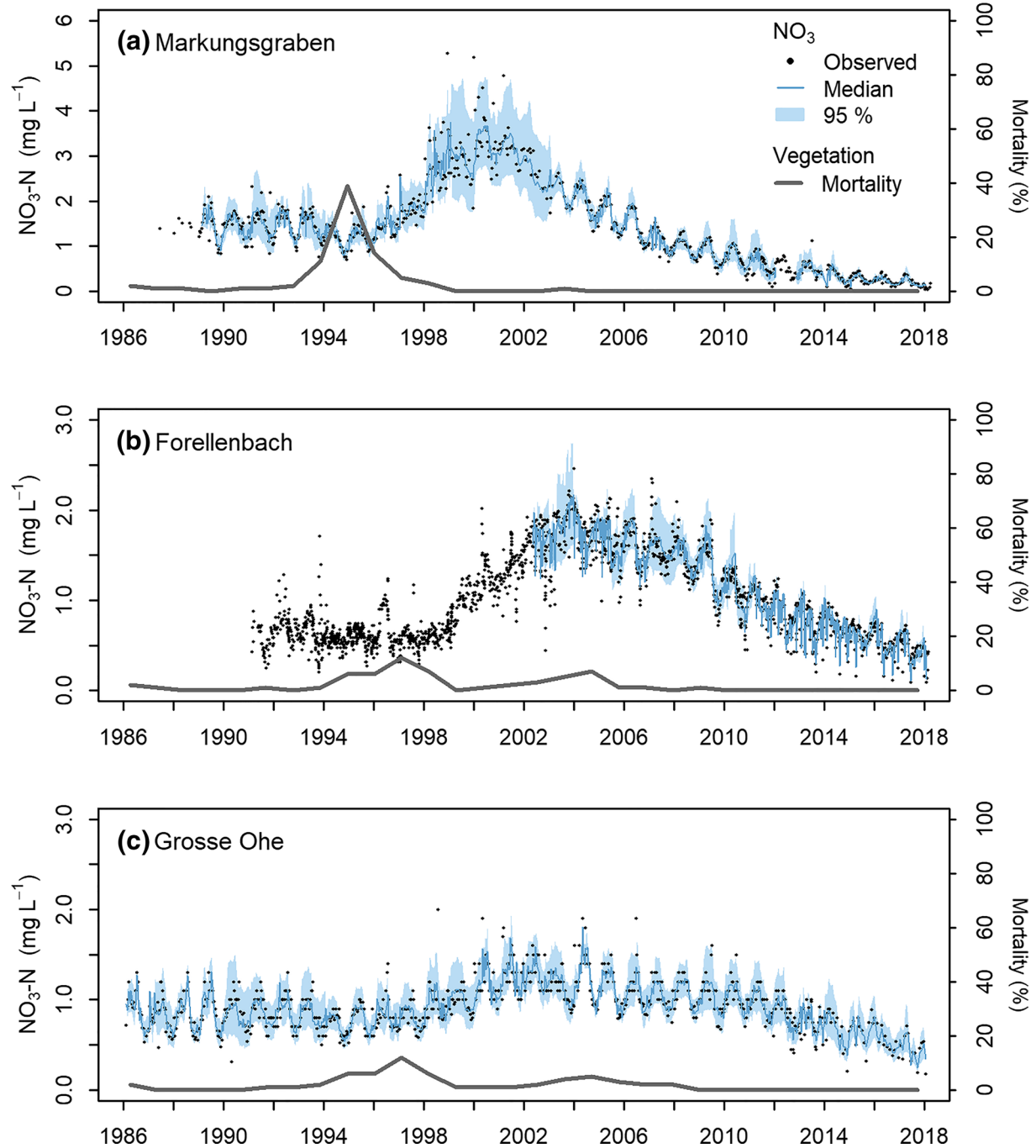
Figure 2. Predicted and observed in-stream nitrate concentrations at the outlets of (a) Markungsgraben, (b) Forellenbach and (c) Grosse Ohe. Vegetation mortalities in the (sub) catchments are indicated as a gray solid line.

showed a larger temporal variation compared to those of the other sites. From 2006 onwards, the kt_r at Markungsgraben was -0.10–$-0.05°C^{-1}$ (range of annual medians), considerably lower than at the other sites. The estimate of kt_r was very uncertain in 2012 (-0.07 [-0.13–-0.02]$°C^{-1}$) because only three data points were available in this year.

The estimates of the C-Q slope b fluctuated near or above zero at Markungsgraben and Grosse Ohe (annual median -0.08–0.21) in their respective predieback and dieback phases (Figure 4c). The medians of
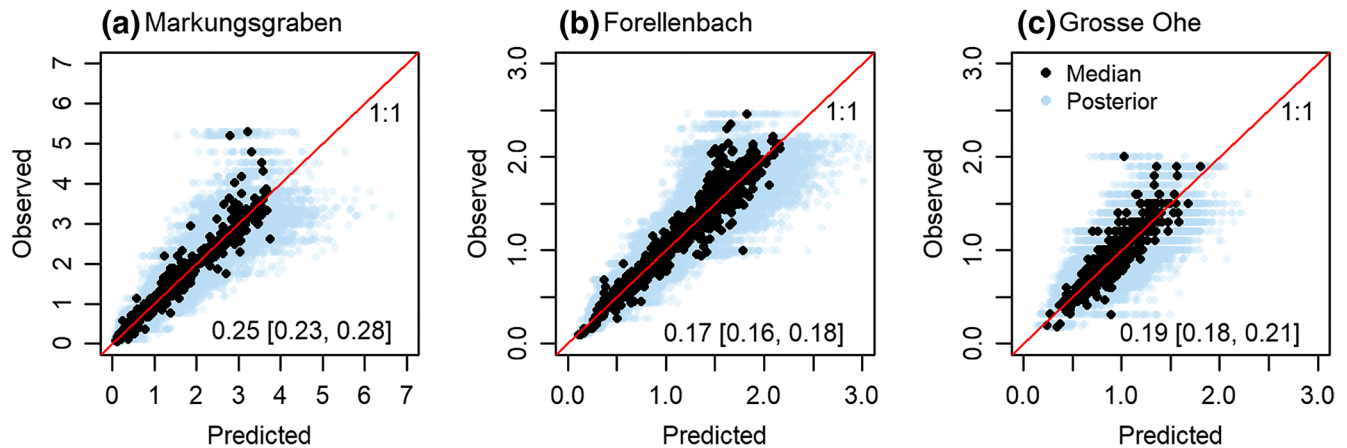
Figure 3. Predicted versus observed in-stream nitrate (NO$_3$) concentration of (a) Markungsgraben, (b) Forellenbach and (c) Grosse Ohe. Posterior distributions and medians of predicted NO$_3$ are displayed. Blue points are random draws from the posterior distribution. 1:1 lines and normalized root mean square errors (median [95% credible interval]) are indicated.

the parameter b decreased below zero in the postdieback phase from 2004 at Markungsgraben and 2012 at Grosse Ohe, although their 95% credible intervals overlapped with zero in some years. At Forellenbach, *b* was clearly negative in all years investigated except for 2007–2009. These years, in which *b* was estimated near or above zero (median −0.05–0.03), are the last years of the dieback phase at this site.

The dynamics of S were broken down into dynamics of c_{s0} using Equation 15 given the annual estimates of *S* and *b* and for various values of q_0/λ as this ratio was not explicitly estimated (Figure 5). Reasonable values for q_0/λ were chosen based on the range of discharges observed at our study sites. The specific runoff maxima at the study sites were 23.8–58.3 mm day^{-1} across the years. Hence, the q_0/λ values were chosen as 20, 40, and 60 mm day^{-1} multiplied by the area of the individual (sub) catchment. The chosen values of q_0/λ represent a conservatively wide range of probable maximum discharges. The parameter c_{s0} is positively related with q_0/λ when $b > 0$ and negatively related when $b < 0$ as Equation 15 implies. Although c_{s0} varied with different assumptions of q_0/λ (differences in median of c_{s0} calculated with the assumptions 0.00–1.61 mg N L^{-1}), the general temporal pattern of c_{s0} was not affected by these assumptions.

The parameter c_{s0} showed a steep increase at the onset of the dieback in Markungsgraben and less alterations in Forellenbach and Grosse Ohe. At Markungsgraben, c_{s0} rose up to 2.66–11.62 mg N L^{-1} in 1998 depending on the assumed q_0/λ. At Forellenbach and Grosse Ohe, c_{s0} remained in the ranges of 0.01–3.27 mg N L^{-1} and 0.01–9.60 mg N L^{-1}, respectively. The c_{s0} estimates of Forellenbach were the lowest among the monitored sites.

The estimated c_{s0} peaked in 1998 at Markungsgraben and Grosse Ohe, preceding the peak of in-stream NO$_3$ (2000 at Markungsgraben and 2003 at Grosse Ohe). Then, c_{s0} decreased below the predieback levels from 2005, 2010 and 2012 onwards at Markungsgraben, Forellenbach and Grosse Ohe, respectively, as the vegetation recovered (Figure 1a). c_{s0} of Markungsgraben showed an especially drastic decrease below predieback levels and even below that of Grosse Ohe.

The c_{s0} estimated with $q_0/\lambda = 40$, as an example, was correlated with the annual mean of in-stream NO$_3$ with a ρ of 0.88 (0.81, 0.92) at Markungsgraben, 0.77 (0.74, 0.80) at Forellenbach and 0.70 (0.61, 0.79) at Grosse Ohe. c_{s0} tended to be higher than in-stream NO$_3$ until 2004 at Markungsgraben and until 2012 at Grosse Ohe and was similar or lower afterward at both sites. At Forellenbach, c_{s0} was lower than in-stream NO$_3$ for most of the research period except in 2007–2009, when they were comparable to each other.

3.6. Correlations Between Model Parameters and NDVI

The NDVI was negatively correlated with the annual model parameters, most notably c_{s0}, with Spearman's rank correlation coefficients ρ of −0.67 (−0.74, −0.59), −0.81 (−0.85, −0.77) and −0.62 (−0.72, −0.51) at Markungsgraben, Forellenbach and Grosse Ohe, respectively (Figure 6a). The parameter kt$_r$ was negatively
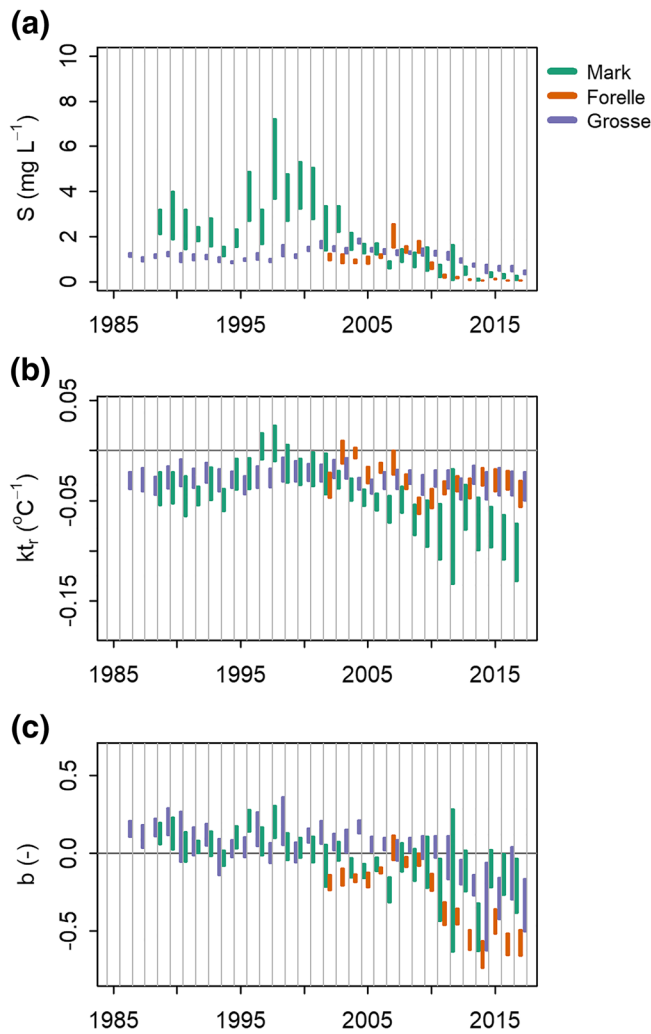
Figure 4. 95% credible intervals of model parameters (a) S, (b) kt_r, and (c) b estimated for each year at Markungsgraben (Mark), Forellenbach (Forelle), and Grosse Ohe (Grosse).

related with NDVI at Markungsgraben and Forellenbach with ρ of -0.70 (-0.78–-0.58) and -0.45 (-0.62–-0.26), respectively (Figure 6b). At Grosse Ohe, the terrestrial vegetation dynamics did not significantly impact kt_r (ρ of -0.10 [-0.34–0.16], with the credible interval including zero). The correlation between the C-Q slope b and NDVI was -0.31 (-0.45–-0.11), -0.81 (-0.86–-0.74) and -0.41 (-0.53–-0.28) at Markungsgraben, Forellenbach and Grosse Ohe, respectively, with the strongest correlation at Forellenbach (Figure 6c).

4. Discussion

4.1. Dynamics of Catchment Processes Inferred via Time-Varying Model Parameters

In the following we interpret the regression parameters by our mechanistic model and discuss what the temporal variations of these parameters mean for catchment processes of N supply via decay of the dead trees and atmospheric deposition, and N removal via hydrological export and biological retention.

4.1.1. Nitrate Inputs to the Soil

The parameter S is highly correlated with the annual mean of stream NO_3 (Section 3.5) since logS is equivalent to the intercept of the regression Equation 6 and annual slopes remain in ranges around zero across the sites ($-0.15 < kt_r < 0.05$ and $-0.8 < b < 0.7$; Figure 4). c_{s0}, the concentration of NO_3 at the soil surface available for export, is proportional to S via Equation 15. The vertical profile of NO_3 export can be inferred if further information on q_0 and λ are available. c_{s0} increased as N was released from the dead trees in the dieback phase and decreased in the postdieback phase again below predieback levels (Figures 1a and 1c). c_{s0} showed negative correlation with NDVI (Figure 6a). These results suggest that the NO_3 input to soils was affected by the vegetation dynamics. Since c_{s0} showed high correlations with the annual mean NO_3 concentration via S, we can infer that the NO_3 input to soils governed strongly the in-stream NO_3 concentration.

The reduction of c_{s0} in the postdieback phase indicates that removal of NO_3 (hydrological export and biological retention) outran supply of NO_3 (decay of the dead tr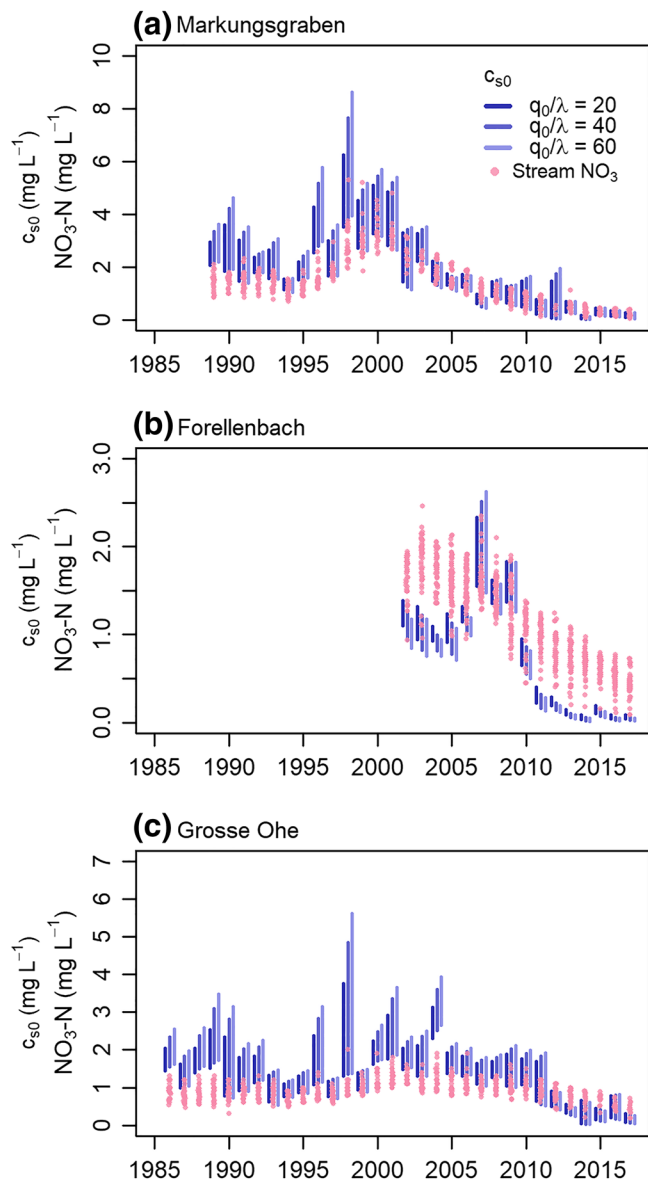ees and atmospheric deposition). The N input via atmospheric deposition showed a reduction over time in our catchment (Beudert & Gietl, 2015). However, since N concentration in the deposition did not show any seasonal pattern and do not correspond to the stream NO_3 dynamics (Figure S2), we can assume that biogeochemical reactions had a stronger influence on in-stream NO_3 than the deposition. Export of NO_3 via stream discharge depleted the nutrient over the course of 7–10 years after the diebacks. Additionally, regrowth of young vegetation enhanced net retention of NO_3 as it shed little amounts of litter compared to mature vegetation (Bormann & Likens, 1994; Covington, 1979). The strongest dieback in Markungsgraben created large openings and allowed for the establishment and growth of understory vegetation communities (Niemelä, 1999), which likely led to the most active regrowth of the vegetation (Figure 1a) and reduction of c_{s0} (Figure 5) in this subcatchment.

For comparison, the NO_3 concentration in soil water measured in the Forellenbach catchment by Beudert and Klöcking (2007) rose in 1997–2000 up to approximately 45 mg N L^{-1}, 12-fold higher than the maximum c_{s0} estimated at this site (Figure 5). Soil water in that study was collected from a plot with a dead spruce stand upslope of the stream, while c_{s0} in this study conceptually represents the lumped NO_3 concentration at the soil surface of the whole catchment including soils that were not affected by the bark beetle infestation. The model might have also underestimated the soil surface NO_3 concentration as input and export of the nutrient were not explicitly estimated as data and the nutrient was exported at a high rate. Providing

Figure 5. 95% credible intervals of concentration of nitrate (NO_3) input to soils (c_{s0}) compared with stream NO_3 concentration at (a) Markungsgraben, (b) Forellenbach and (c) Grosse Ohe. Three c_{s0} scenarios are shown based on different q_0/λ values and all convey a similar pattern.

data of effective NO_3 distribution in the soil of the entire catchment as a boundary condition could remove this ambiguity and result in different estimations (Musolff et al., 2016).

4.1.2. Rates of Biogeochemical Processes

The temporal evolution of NO_3 concentrations and the biogeochemical reaction parameter kt_r in our study catchment reflects how its N budget evolved during the bark beetle outbreak and the subsequent succession. We conceptualize mineralization and nitrification as production and plant and microorganism assimilation and denitrification as retention, which take place mostly in the near-surface layer. The parameter kt_r was negative in the predieback period, indicating that the catchment was a net sink of NO_3. With the dieback, NO_3 was produced at a rate comparable to that of its retention in the catchment ($kt_r \approx 0$ C°$^{-1}$). The catchment started to retain NO_3 effectively again in the postdieback phase, showing negative kt_r.

Vegetation controls N export not only by taking up the nutrient for growth but also by providing a carbon energy source via exudation or litterfall for microbial denitrification (Dosskey et al., 2010; Mulholland et al., 2008; Scaglia et al., 1985; Zhai et al., 2013). Carbon was released from the litterfall when the trees were killed and might have enhanced denitrification (Biederman et al., 2016; Mikkelson et al., 2013). However, the permeable soil in the catchment is not favorable to denitrification (Beudert et al., 2014). A kt_r near zero implies that the denitrification was not so significantly enhanced that it did not outrun the increased NO_3 production from the N release. Furthermore, nutrient uptake and carbon exudation could have been impaired by the mortality of the trees and recovered with the forest recovery, supported by the correlation between kt_r and NDVI especially in the strongly affected Markungsgraben. While denitrification has been reported as the primary process of NO_3 removal in some soil-water systems (Bachand & Horne, 1999; Mulholland et al., 2008), in landscapes of high precipitation and undisturbed permeable soils, which cover about 70% of our catchment, denitrification losses have been shown to be small compared to retention by uptake (Oertel, 2020). Hence Huber (2005) attributed the seasonal pattern of NO_3 in our catchment to the active vegetation uptake during summer. It was not possible to separate the two pathways of retention with the data available for this study to provide a new perspective on these findings.

With marginal changes in annual precipitation, evapotranspiration was reduced while the runoff coefficient increased in the catchments following the dieback, most remarkable in Markungsgraben (Bernsteinová et al., 2015; Beudert & Klöcking, 2007). The increased runoff coefficient suggests that canopy mortality could have altered the residence time of the nutrient in the near-surface layer (t_r) and thus affected the N retention capacity (Hill et al., 1998). However, this effect could not be separated from the parameter kt_r in our study.

To explain the increased production during the dieback phase ($kt_r > 0$ C°$^{-1}$), we suggest that organic N and ammonium (NH_4) released from the killed trees were available for mineralization and nitrification, from which more NO_3 was produced in the growing season at high temperatures (Arheimer et al., 1996; Kaiser et al., 2011). When kt_r was near zero across the sites, the production and removal of NO_3 in the near-surface layer were of comparable rates so the in-stream NO_3 concentration did not show a seasonal pattern. Such disappearance or even reversal of the seasonal pattern after severe dieback due to increased NO_3 production has frequently been observed in forest catchments (Kaňa et al., 2015; Pardo et al., 1995; Yeakley et al., 2003).
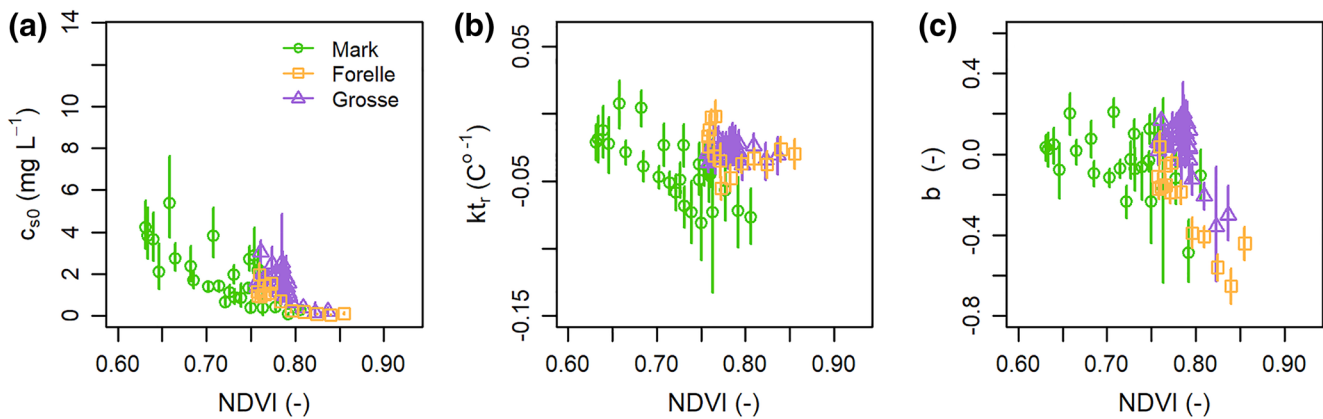
Figure 6. Annual model parameter estimates (a) c_{s0}, (b) b and (c) kt_r for Markungsgraben (Mark), Forellenbach (Forelle) and Grosse Ohe (Grosse) plotted against NDVI. Error bars signify the 95% credible intervals of the parameters.

4.1.3. Hydrological Pathways of Nitrate Export

The C-Q relationship which is part of the regression model employed here has been interpreted by heterogeneous nutrient sources within a catchment that are variously connected to the stream by dynamic transport pathways (Basu et al., 2010; Seibert et al., 2009). Looking at the regression model parameters in a mechanistic sense, $b > 0$ indicates nutrient flushing with increasing flow (see Equation 14), indicative of active near-surface pathways intersecting nutrient-rich layers. Conversely, $b < 0$ indicates nutrient dilution with increasing flow, indicative of near-surface pathways that dilute near-surface sources. A value for b near zero indicates that the solute transport is homogeneous over the depth of the soil and does not vary with discharge (chemostasis). Godsey et al. (2009) connected chemostatic export of geogenic solutes with b values in the range of (−0.2, 0.2). Basu et al. (2010) found similar chemostatic export for NO_3 in a N-saturated catchment. The C-Q relationship can vary if the dominant pathway of nutrient export is switched (Zhi et al., 2019). In our catchment, the temporal variations of b and c_{s0} suggest that the NO_3 export was chemostatic in the predieback and dieback phases and shifted to a dilution pattern in the postdieback period.

The parameter b was in the range of (−0.2, 0.2) at Markungsgraben and Grosse Ohe in most of the predieback phase (Figure 4c) indicating chemostasis of the NO_3 export. Several studies observed that chemostasis of NO_3 is a sign of N-saturation with the nutrient homogeneously transported (Basu et al., 2010; Bieroza et al., 2018; Van Meter & Basu, 2015). The parameter b and kt_r were near zero when the parameter c_{s0} was estimated comparable to in-stream NO_3 (1999–2002 in Markungsgraben and 2007–2009 in Forellenbach), which is mixture of the nutrient exported from the soil profile, supporting indirectly that NO_3 transport was homogeneous in the soil profile (Figures 4 and 5). Conversely, b was slightly above zero when c_{s0} was higher than in-stream NO_3. The parameters b and c_{s0} were especially high in the dieback phase (Figures 4a and 4c) showing high correlations with NDVI (Figure 6c). In these years, NO_3 released from the killed trees likely accumulated in the near-surface layer inducing a flushing effect and hence steep increases in c_{s0} and b.

The parameter b decreased below zero (Figure 4) and c_{s0} was lower than the stream NO_3 (Figure 5) in the postdieback phase (after 2014 at Markungsgraben and after 2013 at Grosse Ohe). We suggest, by that time, the NO_3 concentration in the near-surface layer had been depleted by the flushing and the biological retention although the data did not allow a quantification of the N budget of the catchment. It is also likely that the NO_3 had leached into deeper groundwater over time during and after the diebacks (Jury & Nielsen, 1989). The water flux through the near-surface layer at high flows then diluted NO_3 in the stream, resulting in the negative C-Q slopes observed.

The parameter b was lowest at Forellenbach and clearly negative in the pre and postdieback periods, signifying a strong dilution effect in this subcatchment. Indeed, the NO_3 concentration decreased sharply in storm events. This dilution effect is supported by the high baseflow index of 64% possibly caused by comparably flat topography (Section 3.1). In 2007–2009, during the second dieback (Figure 1a), b was near zero and c_{s0} was comparable to in-stream NO_3, likely a sign of N-saturation as discussed above. In the postdieback

phase, b was decreased below zero and predieback levels and c_{s0} was much lower than in-stream NO_3, following a similar pattern to Markungsgraben and Grosse Ohe.

4.2. Concentration-Discharge-Temperature Relationship

Regression modeling predicting NO_3 concentrations in streams from air or water temperature as a single predictor has been used elsewhere (e.g. Clark et al., 2004; Exner-Kittridge et al., 2016). A negative C-T relationship is attributed to reduced microbial and plant uptake of the nutrient at low temperatures (Clark et al., 2004). Winterdahl et al. (2011) revealed that soil temperature was an important factor explaining the residuals of a C-Q model for dissolved organic carbon (DOC). They modified the C-Q model by Seibert et al. (2009) to allow the profile of concentration to vary as a function of soil temperature. The current study found that the C-Q-T model predicted NO_3 export more accurately than either the C-T or the C-Q model (Table S2). The C-Q-T model in this study is also more accurate than the C-Q-S model adapted from the WRTDS model of Hirsch et al. (2010). The mechanistic model developed here (Section 3.3) elucidates the processes behind the empirical C-Q-T relationship, complementing the attempts by Winterdahl et al. (2011) and Hirsch et al. (2010).

Basu et al. (2011) and Thompson et al. (2011) classified solute export from a catchment into source-limited and transport-limited states. Previous studies suggested different metrics for verifying the state of solute export, such as the parameter b, the coefficients of variation (CV) and the coefficient of determination (r^2) of a load-discharge regression (Basu et al., 2010; Godsey et al., 2009; Musolff et al., 2015). In our study, shifts between these states were indicated based on the annual estimates of the parameters kt_r, b and c_{s0} of the C-Q-T model. The NO_3 export arguably was in a transport-limited state in the predieback phase, revealed by its chemostasis ($-0.2 \leq b \leq 0.2$). However, the near-surface layer acted as a net sink of NO_3 ($kt_r < 0$ C$^{\circ-1}$; c_{s0} higher than in-stream NO_3), and in-stream NO_3 was stagnant, indicating an equilibrium between export and retention of NO_3. In the dieback phase, the nutrient export was exacerbated with the release of N from the killed trees (increased c_{s0}) without net retention ($kt_r \approx 0$ C$^{\circ-1}$). As N was depleted and the forest recovered in the postdieback phase (Likens et al., 1978), the nutrient export arguably shifted to a source-limited state with strong N retention (low negative kt_r), NO_3 dilution ($b < 0$) and decreased NO_3 transport in the near-surface layer (lowered c_{s0}).

4.3. Benefits of the Bayesian Hierarchical Approach

Previous studies of the C-Q model revealed that its parameters vary temporally (Hirsch et al., 2010; Köhler et al., 2008; Seibert et al., 2009). The C-Q-T model of our study was fit to the data in a Bayesian hierarchical framework to allow for the annual variability of its parameters, which offered explanations of the temporal changes in the catchment processes caused by the forest dieback. Partial pooling of the annual information as part of the hierarchical approach was especially beneficial for avoiding overfitting, evidenced by enhanced predictive performance compared to the pooled and nonpooled model variants (Table 1; Cha et al., 2016; Simpson, 1951). The effect of partial pooling is evident at Markungsgraben in 2012, where only three data points existed. Here the parameter estimates are shrunk toward their overall means (across years) as the best estimates in the absence of more evidence from that particular year. Following the top-down approach, a logical next level of model development would be the prediction of the parameter variations found here, as Cha et al. (2017) demonstrated, with data of vegetation dynamics, for instance NDVI in our case. It would also be possible to partially pool information in space across catchments (Borsuk et al., 2001; Cha et al., 2016), but this would have to take account of the correlation induced by the nested nature of Markungsgraben, Forellenbach and Grosse Ohe and probably also the effect of stream order.

5. Conclusions

In our forest catchment, the response of stream NO_3 concentration (C) to bark beetle induced forest dieback was best predicted with discharge (Q) and temperature (T). This C-Q-T relationship adds to the widely acknowledged C-Q relationship the effect of temperature on the variability of solutes in streams. The C-Q-T relationship could be applicable to other nonconservative solutes in streams that are regulated by

biogeochemical reactions, and hence are sensitive to temperature. It would be worthwhile to investigate the applicability of the C-Q-T model to different solutes and types of catchments.

The top-down modeling approach yielded mechanistic interpretations of some major hydrochemical processes (soil N inputs, main transport pathways and rates of biogeochemical reactions) in a parsimonious way that is commensurate with the data availability. The model, however, could not explain separate effects of vegetation uptake, denitrification and heterogeneity in biogeochemical reactions and residence time with the available data. The input and export of N were not explicitly evaluated by the model. The flexibility of Bayesian hierarchical modeling is especially suited for top-down modeling via time-varying parameters. Partial pooling maintains flexibility of model parameters while avoiding overfitting. The next step following the top-down route would be to explicitly model the annual variation of parameters by auxiliary data, such as NDVI as indicated in our study.

The temporal trends of the parameters lead us to conclude that the NO_3 released through tree mortality (increased c_{s0}) was not effectively retained in the catchment during the dieback phase ($kt_r \geq 0\ C^{\circ-1}$). In the post-dieback phase, NO_3 was depleted (decreased c_{s0}) and young re-growing vegetation retained more NO_3 than it released N via litter shedding ($kt_r < 0\ C^{\circ-1}$). We attribute the changes in the NO_3 budget to the alteration in the nutrient retention capacity of the catchment but also to abrupt release and depletion of the nutrient.

Although the bark beetle induced forest dieback observed in our study catchment impaired the water quality by releasing N from the forest, the system turned out resilient in the sense of a rapid recovery of ecosystem functions (i.e., retaining nutrients). It is important to note here that the system was not managed at all. Stream NO_3 concentrations were reduced 10 years after the dieback in the most severely affected upper sub-catchment and did not show a drastic response in the most downstream reach (Figure 2). In addition, the biodiversity in our forest catchment was improved after the diebacks with the emergence of new habitats provided by standing and lying deadwood (Beudert et al., 2014). Hence, our study supports the argument that European montane spruce forests are in fact highly resilient to the current disturbance regime (Senf et al., 2019; Zeppenfeld et al., 2015); we here complemented these previous studies by showing that this resilience also includes the key ecosystem function of water purification.

The water temperature in our catchment showed a constantly increasing trend presumably as a manifestation of climate change (Beudert et al., 2018). An increase in forest mortality is expected under climate change (Allen et al., 2010; Seidl et al., 2017), with more frequent forest diebacks that might also increase in severity. Hence, under climate change more nutrients might be released. A portion of the released N would be denitrified and released into the atmosphere as nitrous oxide (N_2O; Norton et al., 2015), a potent greenhouse gas. It would be shortsighted to limit N cycling studies to water quality effects ignoring the climate change potential of N_2O emissions. Further studies are needed to explore the response of the complete N cycle of forest catchments to changing mortality patterns under climate change.

Data Availability Statement

The hydrochemical data were provided from the Bavarian Environment Agency (LFU) and the German Federal Environment Agency (UBA) and are available online in Zenodo repository (https://doi.org/10.5281/zenodo.3703070; Beudert et al., 2020).

References

Adams, H. D., Luce, C. H., Breshears, D. D., Allen, C. D., Weiler, M., Hale, V. C., et al. (2012). Ecohydrological consequences of drought-and infestation-triggered tree die-off: Insights and hypotheses. *Ecohydrology*, *5*(2), 145–159. https://doi.org/10.1002/eco.233

Allen, C. D., Macalady, A. K., Chenchouni, H., Bachelet, D., McDowell, N., Vennetier, M., et al. (2010). A global overview of drought and heat-induced tree mortality reveals emerging climate change risks for forests. *Forest Ecology and Management*, *259*(4), 660–684. https://doi.org/10.1016/j.foreco.2009.09.001

Arheimer, B., Andersson, L., & Lepistö, A. (1996). Variation of nitrogen concentration in forest streams—Influences of flow, seasonality and catchment characteristics. *Journal of Hydrology*, *179*(1–4), 281–304. https://doi.org/10.1016/0022-1694(95)02831-5

Bachand, P. A. M., & Horne, A. J. (1999). Denitrification in constructed free-water surface wetlands: II. Effects of vegetation and temperature. *Ecological Engineering*, *14*(1–2), 17–32. https://doi.org/10.1016/S0925-8574(99)00017-8

Basu, N. B., Destouni, G., Jawitz, J. W., Thompson, S. E., Loukinova, N. V., Darracq, A., et al. (2010). Nutrient loads exported from managed catchments reveal emergent biogeochemical stationarity. *Geophysical Research Letters*, *37*, L23404. https://doi.org/10.1029/2010GL045168

Basu, N. B., Thompson, S. E., Suresh, P., & Rao, C. (2011). Hydrologic and biogeochemical functioning of intensively managed catchments: A synthesis of top-down analyses. *Water Resources Research*, *47*, W00J15. https://doi.org/10.1029/2011WR010800

Bernsteinová, J., Bässler, C., Zimmermann, L., Langhammer, J., & Beudert, B. (2015). Changes in runoff in two neighbouring catchments in the Bohemian Forest related to climate and land cover changes. *Journal of Hydrology and Hydromechanics*, *63*(4), 342–352. https://doi.org/10.1515/johh-2015-0037

Betts, E. F., & Jones Jr, J. B. (2009). Impact of wildfire on stream nutrient chemistry and ecosystem metabolism in boreal forest catchments of interior Alaska. *Arctic, Antarctic, and Alpine Research*, *41*(4), 407–417. http://doi.org/10.1657/1938-4246-41.4.407

Beudert, B., Bässler, C., Thorn, S., Noss, R., Schröder, B., Dieffenbach-Fries, H., et al. (2014). Bark beetles increase biodiversity while maintaining drinking water quality. *Conservation Letters*, *8*(4), 272–281. https://doi.org/10.1111/conl.12153

Beudert, B., Bernsteinová, J., Premier, J., & Bässle, C. (2018). Natural disturbance by bark beetle offsets climate change effects on streamflow in headwater catchments of the Bohemian Forest. *Silva Gabreta*, *24*, 21–45.

Beudert, B., & Gietl, G. (2015). Long-term monitoring in the Große Ohe catchment, Bavarian Forest National Park. *Silva Gabreta*, *21*(1), 5–27.

Beudert, B., Jung, H., Senf, C., & Krueger, T. (2020). Water quality and discharge monitoring data. In *Bavarian Forest National Park*. Germany: Zenodo https://doi.org/10.5281/zenodo.3703070

Beudert, B., & Klöcking, B. (2007). Grosse Ohe: impact of bark beetle infestation on the water and matter budget of a forested catchment. In R. Schwarze, & S. V. Marunich (Eds.), *Forest hydrology: Results of research in Germany and Russia*. Koblenz: IHP/HWRP-Sekretariat.

Biederman, J. A., Meixner, T., Harpold, A. A., Reed, D. E., Gutmann, E. D., Gaun, J. A., & Brooks, P. D. (2016). Riparian zones attenuate nitrogen loss following bark beetle-induced lodgepole pine mortality. *Journal of Geophysical Research: Biogeosciences*, *121*, 933–948. https://doi.org/10.1002/2015JG003284

Bieroza, M. Z., Heathwaite, A. L., Bechmann, M., Kyllmar, K., & Jordan, P. (2018). The concentration-discharge slope as a tool for water quality management. *The Science of the Total Environment*, *630*, 738–749. https://doi.org/10.1016/j.scitotenv.2018.02.256

Bormann, F. H., & Likens, G. (1994). *Pattern and process in a forested ecosystem*. New York: Springer. https://doi.org/10.1007/978-1-4612-6232-9

Borsuk, M. E., Higdon, D., Stow, C. A., & Reckhow, K. H. (2001). A Bayesian hierarchical model to predict benthic oxygen demand from organic matter loading in estuaries and coastal zones. *Ecological Modelling*, *143*, 165–181. https://doi.org/10.1016/S0304-3800(01)00328-3

Botter, G., Basu, N. B., Zanardo, S., Rao, P. S. C., & Rinaldo, A. (2010). Stochastic modeling of nutrient losses in streams: Interactions of climatic, hydrologic, and biogeochemical controls. *Water Resources Research*, *46*, W08509. https://doi.org/10.1029/2009WR008758

Carpenter, B., Gelman, A., Hoffman, M. D., Lee, D., Goodrich, B., Betancourt, M., et al. (2017). Stan: A probabilistic programming language. *Journal of Statistical Software*, *76*(1), 1–32. https://doi.org/10.18637/jss.v076.i01

Cha, Y., K. H. Cho, H. Lee, T. Kang, and J. H. Kim (2017), The relative importance of water temperature and residence time in predicting cyanobacteria abundance in regulated rivers, *Water Research*, *124*, 11–19. http://dx.doi.org/10.1016/j.watres.2017.07.040

Cha, Y., Park, S. S., Lee, H. W., & Stow, C. A. (2016). A Bayesian hierarchical approach to model seasonal algal variability along an upstream to downstream river gradient. *Water Resources Research*, *52*, 348–357. https://doi.org/10.1002/2015WR017327

Chavez, F. P., & Service, S. K. (1996). Temperature-nitrate relationships in the central and eastern tropical Pacific. *Journal of Geophysical Research*, *101*(C9), 20553–20563.

Chen, F.-s., Zeng, D.-h., Narain, S. A., Chen, G.-s., & China, P. R. (2005). Effects of soil moisture and soil depth on nitrogen mineralization process under Mongolian pine plantations in Zhanggutai sandy land. *Journal of Forestry Research*, *16*, 101–104. https://doi.org/10.1007/BF02857899

Christensen, P. B., Nielsen, L. P., Sørensen, J., & Revsbech, N. P. (1990). Denitrification in nitrate-rich streams: Diurnal and seasonal variation related to benthic oxygen metabolism. *Limnology and Oceanography*, *35*(3), 640–651. https://doi.org/10.4319/lo.1990.35.3.0640

Clark, M. J., Cresser, M. S., Smart, R., Chapman, P. J., & Edwards, A. C. (2004). The influence of catchment characteristics on the seasonality of carbon and nitrogen species concentrations in upland rivers of Northern Scotland. *Biogeochemistry*, *68*, 1–19. https://doi.org/10.1023/B:BIOG.0000025733.07568.11

Covington, W. W. (1979). *Forest floor organic matter and nutrient content and leaf fall during secondary succession in northern hardwoods* (p. 99). New Haven, CT: Yales University.

Dosskey, M. G., Vidon, P., Gurwick, N. P., Allan, C. J., Duval, T. P., & Lowrance, R. (2010). The role of riparian vegetation in protecting and improving chemical water quality in streams. *Journal of the American Water Resources Association*, *46*(2), 261–277.

Fuka, D. R., Walter, M. T., Archibald, J. A., Steenhuis, T. S. & Easton, Z. M. (2018). EcoHydRology: A Community Modeling Foundation for Eco-Hydrology. *R package version 0.4.12.1*. Retrieved from https://CRAN.R-project.org/package=EcoHydRology

Exner-Kittridge, M., Strauss, P., Bl, C. n., schl, A. E., E. S., & Zessner, M. (2016). The seasonal dynamics of the stream sources and input flow paths of water and nitrogen of an Austrian headwater agricultural catchment. *The Science of the Total Environment*, *542*, 935–945. http://dx.doi.org/10.1016/j.scitotenv.2015.10.151

Gall, H. E., Park, J., Harman, C. J., Jawitz, J. W., & Rao, P. S. C. (2013). Landscape filtering of hydrologic and biogeochemical responses in managed catchments. *Landscape Ecology*, *28*, 651–664. https://doi.org/10.1007/s10980-012-9829-x

Gelman, A. (2006). Prior distributions for variance parameters in hierarchical models (comment on article by Browne and Draper). *Bayesian analysis*, *1*(3), 515–534. https://doi.org/10.1214/06-BA117A

Godsey, S. E., Kirchner, J. W., & Clow, D. W. (2009). Concentration–discharge relationships reflect chemostatic characteristics of US catchments. *Hydrological Processes: International Journal*, *23*(13), 1844–1864. https://doi.org/10.1002/hyp.7315

Gorham, E., Vitousek, P. M., & Reiners, W. A. (1979). The regulation of chemical budgets over the course of terrestrial ecosystem succession. *Annual Review of Ecology and Systematics*, *10*(1), 53–84. https://doi.org/10.1146/annurev.es.10.110179.000413

Gundersen, P., Schmidt, I. K., & Raulund-Rasmussen, K. (2006). Leaching of nitrate from temperate forests effects of air pollution and forest management. *Environmental Reviews*, *14*(1), 1–57. https://doi.org/10.1139/a05-015

Hais, M., Jonášová, M., Langhammer, J., & Kučera, T. (2009). Comparison of two types of forest disturbance using multitemporal Landsat TM/ETM+ imagery and field vegetation data. *Remote Sensing of Environment*, *113*, 835–845. https://doi.org/10.1016/j.rse.2008.12.012

Hansen, M. C., Potapov, P. V., Moore, R., Hancher, M., Turubanova, S. A., Tyukavina, A., et al. (2013). High-resolution global maps of 21st-century forest cover change. *Science*, *342*, 850–853. https://doi.org/10.1126/science.1244693

Harman, C. J., Rao, P. S. C., Basu, N. B., McGrath, G. S., Kumar, P., & Sivapalan, M. (2011). Climate, soil, and vegetation controls on the temporal variability of vadose zone transport. *Water Resources Research*, *47*, W00J13. https://doi.org/10.1029/2010WR010194

Hartmann, A., Kobler, J., Kralik, M., Dirnböck, T., Humer, F., & Weiler, M. (2016). Model-aided quantification of dissolved carbon and nitrogen release after windthrow disturbance in an Austrian karst system. *Biogeosciences*, *131*, 159–174. https://doi.org/10.5194/bg-13-159-2016

Heurich, M., Ochs, T., Andresen, T., & Schneider, T. (2010). Object-orientated image analysis for the semi-automatic detection of dead trees following a spruce bark beetle (*Ips typographus*) outbreak. *European Journal of Forest Research*, *129*(3), 313–324. https://doi.org/10.1007/s10342-009-0331-1

Hill, A. R., Labadia, C. F., & Sanmugadas, K. (1998). Hyporheic zone hydrology and nitrogen dynamics in relation to the streambed topography of a N-rich stream. *Biogeochemistry*, *42*(3), 285–310. https://doi.org/10.1023/A:1005932528748

Hilton, J., O'Hare, M., Bowes, M. J., & Jones, J. I. (2006). How green is my river? A new paradigm of eutrophication in rivers. *The Science of the Total Environment*, *365*(1–3), 66–83. https://doi.org/10.1016/j.scitotenv.2006.02.055

Hirsch, R. M., Moyer, D. L., & Archfield, S. A. (2010). Weighted regressions on time, discharge, and season (WRTDS), with an application to Chesapeake Bay river inputs 1. *JAWRA Journal of the American Water Resources Association*, *46*(5), 857–880. https://doi.org/10.1111/j.1752-1688.2010.00482.x

Hlásny, T., Krokene, P., Liebhold, A., Montagné-Huck, C., Müller, J., Qin, H., et al. (2019). In L. Hetemäki (Ed.), *Living with bark beetles: Impacts, outlook and management options*. Joensuu: European Forest Institute.

Huber, C. (2005). Long lasting nitrate leaching after bark beetle attack in the highlands of the Bavarian Forest National Park. *Journal of Environmental Quality*, *34*(5), 1772–1779. https://doi.org/10.2134/jeq2004.0210

Jury, W. A., & Nielsen, D. R. (1989). Nitrate transport and leaching mechanisms. In R. F. Follett (Ed.), *Developments in agricultural and managed forest ecology* (pp. 139–157). London: Elsevier.

Kaiser, C., Fuchslueger, L., Koranda, M., Gorfer, M., Stange, C. F., Kitzler, B., et al. (2011). Plants control the seasonal dynamics of microbial N cycling in a beech forest soil by belowground C allocation. *Ecology*, *92*(5), 1036–1051. https://doi.org/10.1890/10-1011.1

Kautz, M., Dworschak, K., Gruppe, A., & Schopf, R. (2011). Quantifying spatio-temporal dispersion of bark beetle infestations in epidemic and non-epidemic conditions. *Forest Ecology and Management*, *262*(4), 598–608. https://doi.org/10.1016/j.foreco.2011.04.023

Kaňa, J., Tahovská, K., Kopáček, J., & Šantrůčková, H. (2015). Excess of organic carbon in mountain spruce forest soils after bark beetle outbreak altered microbial N transformations and mitigated N-saturation. *PloS One*, *10*(7), e0134165. https://doi.org/10.1371/journal.pone.0134165

Köhler, S. J., Buffam, I., Laudon, H., & Bishop, K. H. (2008). Climate's control of intra-annual and interannual variability of total organic carbon concentration and flux in two contrasting boreal landscape elements. *Journal of Geophysical Research: Biogeosciences*, *113*(G3), G03012. https://doi.org/10.1029/2007JG000629

Krueger, T., Freer, J., Quinton, J. N., & Macleod, C. J. A. (2007). Processes affecting transfer of sediment and colloids, with associated phosphorus, from intensively farmed grasslands: a critical note on modelling of phosphorus transfers. *Hydrological Processes*, *21*, 557–562. https://doi.org/10.1002/hyp.6596

Lajtha, K. (2020). Nutrient retention and loss during ecosystem succession: Revisiting a classic model. *Ecology*, *101*(1), e02896. https://doi.org/10.1002/ecy.2896

Likens, G. E., Bormann, F. H., Pierce, R. S., & Reiners, W. A. (1978). Recovery of a deforested ecosystem. *Science*, *199*(4328), 492–496. https://doi.org/10.1126/science.199.4328.492

Mikkelson, K. M., Bearup, L. A., Maxwell, R. M., Stednick, J. D., McCray, J. E., & Sharp, J. O. (2013). Bark beetle infestation impacts on nutrient cycling, water quality and interdependent hydrological effects. *Biogeochemistry*, *115*(1–3), 1–21. https://doi.org/10.1007/s10533-013-9875-8

Mulholland, P. J., Helton, A. M., Poole, G. C., Hall Jr, R. O., Hamilton, S. K., Peterson, B. J., et al. (2008). Stream denitrification across biomes and its response to anthropogenic nitrate loading. *Nature Letters*, *452*(7184), 202. https://doi.org/10.1038/nature06686

Musolff, A., Schmidt, C., Rode, M., Lischeid, G., Weise, S. M., & Fleckenstein, J. H. (2016). Groundwater head controls nitrate export from an agricultural lowland catchment. *Advances in Water Resources*, *96*, 95–107. https://doi.org/10.1016/j.advwatres.2016.07.003

Musolff, A., Schmidt, C., Selle, B., & Fleckenstein, J. H. (2015). Catchment controls on solute export. *Advances in Water Resources*, *86*, 133–146. https://doi.org/10.1016/j.advwatres.2015.09.026

Niemelä, J. (1999). Management in relation to disturbance in the boreal forest. *Forest Ecology and Management*, *115*(2–3), 127–134. https://doi.org/10.1016/S0378-1127(98)00393-4

Norton, U., Ewers, B. E., Borkhuu, B., Brown, N. R., & Pendall, E. (2015). Soil nitrogen five years after bark beetle infestation in lodgepole pine forests. *Soil Science Society of America Journal*, *79*(1), 282–293. http://10.2136/sssaj2014.05.0233

Obenour, D. R., Gronewold, A. D., Stow, C. A., & Scavia, D. (2014). Using a Bayesian hierarchical model to improve Lake Erie cyanobacteria bloom forecasts. *Water Resources Research*, *50*, 7847–7860. https://doi.org/10.1002/2014WR015616

Oertel, C., Wellbrock, N., Hoffmann, M., & Augustin, J. (2020). *Denitrification as a part of the calculation of critical loads. Paper presented at ICP M&M Task Force Meeting.*

Pardo, L. H., Driscoll, C. T., & Likens, G. E. (1995). Patterns of nitrate loss from a chronosequence of clear-cut watersheds. *Water, Air, and Soil Pollution*, *85*(3), 1659–1664. https://doi.org/10.1007/BF00477218

Pregitzer, K. S., & J. S. King (2005). Effects of soil temperature on nutrient uptake. In B. Hormoz (Ed.), *Nutrient acquisition by plants* (pp. 277–310). Berlin: Springer.

R Core Team (2018). *R: A language and environment for statistical computing*. Vienna: R Foundation for Statistical Computing. Retreived from https://www.R-project.org/

Rose, L. A., Karwan, D. L., & Godsey, S. E. (2018). Concentration–discharge relationships describe solute and sediment mobilization, reaction, and transport at event and longer timescales. *Hydrological Processes*, *32*(18), 2829–2844. https://doi.org/10.1002/hyp.13235

Scaglia, J., Lensi, R., & Chalamet, A. (1985). Relationship between photosynthesis and denitrification in planted soil. *Plant and Soil*, *84*(1), 37–43. https://doi.org/10.1007/BF02197865

Schelhaas, M. J., Nabuurs, G. J., & Schuck, A. (2003). Natural disturbances in the European forests in the 19th and 20th centuries. *Global Change Biology*, *9*, 1620–1633. https://doi.org/10.1046/j.1365-2486.2003.00684.x

Seibert, J., Grabs, T., Köhler, S., Laudon, H., Winterdahl, M., & Bishop, K. (2009). Linking soil- and stream-water chemistry based on a riparian flow-concentration integration model. *Hydrology and Earth System Sciences*, *13*, 2287–2297. https://doi.org/10.5194/hessd-6-5603-2009

Seidl, R., Thom, D., Kautz, M., Martin-Benito, D., Peltoniemi, M., Vacchiano, G., et al. (2017). Forest disturbances under climate change. *Nature Climate Change*, *7*(6), 395. http://10.1038/nclimate3303

Seidl, R., Schelhaas, M.-J., Rammer, W., & Verkerk, P. J. (2014). Increasing forest disturbances in Europe and their impact on carbon storage. *Nature Climate Change*, *4*(9), 806–810. https://doi.org/10.1038/nclimate2318

Senf, C., Müller, J., & Seidl, R. (2019). Post-disturbance recovery of forest cover and tree height differ with management in Central Europe. *Landscape Ecology*, *34*(12), 2837–2850. https://doi.org/10.1007/s10980-019-00921-9

Senf, C., Pflugmacher, D., Hostert, P., & Seidl, R. (2017). Using Landsat time series for characterizing forest disturbance dynamics in the coupled human and natural systems of Central Europe. *ISPRS Journal of Photogrammetry and Remote Sensing*, *130*, 453–463. https://doi.org/10.1016/j.isprsjprs.2017.07.004

Senf, C., & Seidl, R. (2018). Natural disturbances are spatially diverse but temporally synchronized across temperate forest landscapes in Europe. *Global Change Biology*, *24*(3), 1201–1211. https://doi.org/10.1111/gcb.13897

Simpson, E. H. (1951). The interpretation of interaction in contingency tables. *Journal of the Royal Statistical Society: Series B*, *13*(2), 238–241. https://doi.org/10.1111/j.2517-6161.1951.tb00088.x

Sivapalan, M., Blöschl, G., Zhang, L., & Vertessy, R. (2003). Downward approach to hydrological prediction. *Hydrological Processes*, *17*(11), 2010–2111. https://doi.org/10.1002/hyp.1426

Stan Development Team (2018). *Stan development Team. 2018. RStan: The R interface to Stan. R package version 2.17.3*. Retreived from http://mc-stan.org

Stoddard, J. L. (1994). Long-term changes in watershed retention of nitrogen: its causes and aquatic consequences. In L. A. Baker (Ed.), *Environmental chemistry of lakes and reservoirs* (pp. 223–284). ACS Advances in Chemistry Series. http://10.1021/ba-1994-0237.ch008

Stow, C. A., & Scavia, D. (2008). Modeling hypoxia in the Chesapeake Bay: ensemble estimation using a Bayesian hierarchical model. *Journal of Marine Systems*, *76*(1–2), 244–250. https://doi.org/10.1016/j.jmarsys.2008.05.008

Svoboda, M., Fraver, S., Janda, P., Bače, R., & Zenáhlíková, J. (2010). Natural development and regeneration of a Central European montane spruce forest. *Forest Ecology and Management*, *260*(5), 707–714. https://doi.org/10.1016/j.foreco.2010.05.027

Thompson, S. E., Basu, N. B., Lascurain, J., Jr, Aubeneau, A., & Rao, P. S. C. (2011). Relative dominance of hydrologic versus biogeochemical factors on solute export across impact gradients. *Water Resources Research*, *47*, W00J05. https://doi.org/10.1029/2010WR009605

Van Meter, K. J., & Basu, N. B. (2015). Catchment legacies and time lags: A parsimonious watershed model to predict the effects of legacy storage on nitrogen export. *PLoS One*, *10*(5), e0125971. https://doi.org/10.1371/journal.pone.0125971

Vehtari, A., Gelman, A., & Gabry, J. (2017). Practical Bayesian model evaluation using leave-one-out cross-validation and WAIC. *Statistics and Computing*, *27*(5), 1413–1432. http://dx.doi.org/10.1007/s11222-016-9709-3

Vitousek, P. M., & Reiners, W. A. (1975). Ecosystem succession and nutrient retention: A hypothesis. *BioScience*, *25*(6), 376–381. https://doi.org/10.2307/1297148

Webb, J. A., Ardson, M. J. S., & Koster, W. M. (2010). Detecting ecological responses to flow variation using Bayesian hierarchical models. *Freshwater Biology*, *55*, 108–126. https://doi.org/10.1111/j.1365-2427.2009.02205.x

Wetzel, R. (2001). *Limnology: Lake and river ecosystems* (3rd ed.). San Diego, CA: Academic Press. https://doi.org/10.1016/C2009-0-02112-6.

Winterdahl, M., Futter, M., Köhler, S., Laudon, H., Seibert, J., & Bishop, K. (2011). Riparian soil temperature modification of the relationship between flow and dissolved organic carbon concentration in a boreal stream. *Water Resources Research*, *47*(8), W08532. https://doi.org/10.1029/2010WR010235

Xia, Y., Weller, D. E., Williams, M. N., Jordan, T. E., & Yan, X. (2016). Using Bayesian hierarchical models to better understand nitrate sources and sinks in agricultural watersheds. *Water Research*, *105*, 527–539. http://dx.doi.org/10.1016/j.watres.2016.09.033

Xu, H., Paerl, H. W., Qin, B., Zhu, G., Hall, N. S., & Wu, Y. (2014). Determining critical nutrient thresholds needed to control harmful cyanobacterial blooms in eutrophic Lake Taihu, China. *Environmental Science and Technology*, *49*(2), 1051–1059. https://doi.org/10.1021/es503744q

Yeakley, J. A., Coleman, D. C., Haines, B. L., Kloeppel, B. D., Meyer, J. L., Swank, W. T., et al. (2003). Hillslope nutrient dynamics following upland riparian vegetation disturbance. *Ecosystems*, *6*(2), 154–167. https://doi.org/10.1007/s10021-002-0116-6

Zeppenfeld, T., Svoboda, M., DeRose, R. J., Heurich, M., Müller, J., Čížková, P., et al. (2015). Response of mountain Picea abies forests to stand-replacing bark beetle outbreaks: neighbourhood effects lead to self-replacement. *Journal of Applied Ecology*, *52*(5), 1402–1411. https://doi.org/10.1111/1365-2664.12504

Zhai, X., N. Piwpuan, C. A. Arias, T. Headley, & H. Brix (2013), Can root exudates from emergent wetland plants fuel denitrification in subsurface flow constructed wetland systems?, *Ecological Engineering*, *61*(Part B), 555–563. https://doi.org/10.1016/j.ecoleng.2013.02.014

Zheng, L., Bayani, M., Cardenas, & Wang, L. (2016). Temperature effects on nitrogen cycling and nitrate removal-production efficiency in bed form-induced hyporheic zones. *Journal of Geophysical Research: Biogeosciences*, *121*, 1086–1103. http://dx.doi.org/10.1002/2015JG003162

Zhi, W., Li, L., Dong, W., Brown, W., Kaye, J., Steefel, C., & Williams, K. H. (2019). Distinct source water chemistry shapes contrasting concentration-discharge patterns. *Water Resources Research*, *55*, 4233–4251. https://doi.org/10.1029/2018WR024257